

Supporting Information

Nondoped Organic Light-Emitting Diodes with Low Efficiency Roll-Off: Combination of Aggregation-Induced Emission, Hybridized Local and Charge-Transfer State as well as High Photoluminescence Efficiency

Sheng-Yi Yang¹, Yuan-Lan Zhang¹, Aziz Khan¹, You-Jun Yu¹, Sarvendra Kumar¹,
Zuo-Quan Jiang^{1*}, and Liang-Sheng Liao^{1, 2*}

¹ Institute of Functional Nano & Soft Materials (FUNSOM), Jiangsu Key Laboratory for Carbon-Based Functional Materials & Devices, Soochow University, Suzhou, Jiangsu 215123, China.

² Institute of Organic Optoelectronics, Jiangsu Industrial Technology Research Institute (JITRI), Wujiang, Suzhou, Jiangsu 215211, China

E-mail: zqjiang@suda.edu.cn; lsiao@suda.edu.cn.

Contents

- 1. Experimental Section.**
- 2. Supplemental Figures.**
- 3. Supplemental Tables.**
- 4. References.**

Experimental Section

Materials and instruments:

All chemicals and reagents were used as received from commercial sources without further purification. THF and toluene used in synthetic routes were purified by PURE SOLV (Innovative Technology) purification system. ^1H NMR and ^{13}C NMR spectra were recorded on a Bruker 400 spectrometer or Bruker 600 spectrometer at room temperature. UV-Vis absorption spectra were recorded on a Perkin Elmer Lambda 750 spectrophotometer. PL spectra and phosphorescent spectra were recorded on a Hitachi F-4600 fluorescence spectrophotometer. AIEE properties are based on the work of Tang. Differential scanning calorimetry (DSC) was performed on a TA DSC 2010 unit at a heating rate of $10\text{ }^\circ\text{C min}^{-1}$ under nitrogen. The glass transition temperatures (T_g) were determined from the second heating scan. Thermogravimetric analysis (TGA) was performed on a TA SDT 2960 instrument at a heating rate of $10\text{ }^\circ\text{C min}^{-1}$ under nitrogen, temperature at 5% weight loss was used as the decomposition temperature (T_d). DFT and T calculations were performed utilizing B3LYP/6–31G(D) atomic basis set. Cyclic voltammetry(CV) was performed on a CHI 630 electrochemical work station with a scan rate of 100 mV S^{-1} at room temperature (RT) under an argon flow, in which a Pt disk, a Pt plate and a Ag/AgCl electrode were used as working electrode, counter electrode and reference electrode in tetra-*n*-butylammonium hexa-fluorophosphates ($n\text{-Bu}_4\text{NPF}_6$, 0.1 M) acetonitrile solution, respectively. For calibration, the redox potential of ferrocene/ferrocenium(Fc/Fc^+) was measured under the same conditions. The PLQY

was measured using Hamamatsu C9920-02G in nitrogen or air atmosphere. Transient spectra were obtained by using Quantaaurus-Tau fluorescence lifetime measurement system (C11367-03, Hamamatsu Photonics Co.) in vacuum or nitrogen atmosphere.

Single crystal information:

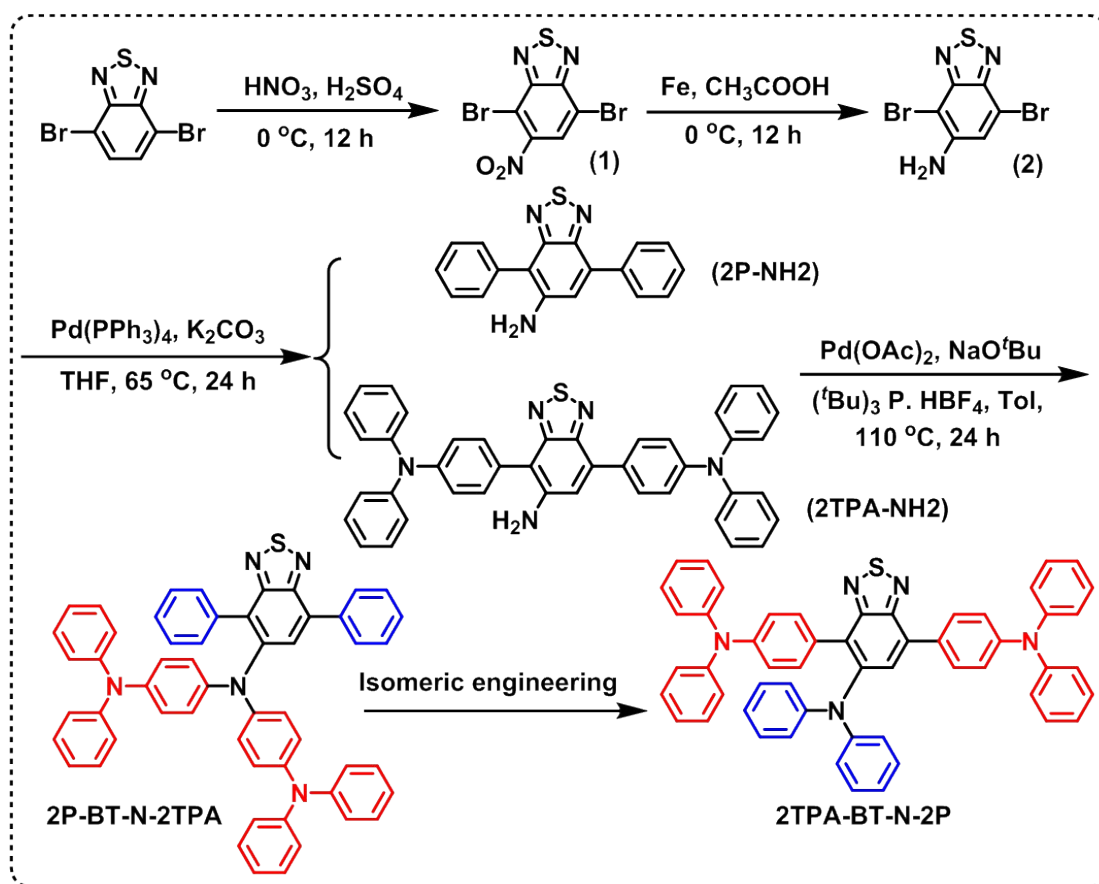
Data collections were performed on a Bruker D8-Venture diffractometer with a Turbo X-ray Source (Mo–K α radiation, $\lambda = 0.71073$ Å) adopting the direct drive rotating anode technique and a CMOS detector at room temperature. The data frames were collected using the program APEX2 and processed using the program SAINT routine in APEX2. The structures were solved by direct methods and refined by the full-matrix least squares on F² using the SHELXTL-2014 program.

Devices fabrication process:

OLEDs were fabricated on ITO glass substrates layer (110 nm, 15 Ω /square) under a base pressure of 3×10^{-6} Torr. The active area of each device is 0.09 cm². Deposition rates and thicknesses of all materials were monitored with oscillating quartz crystals. Doping layers were deposited by utilizing two different sensors to monitor the deposition rates of both host material and dopant material. The deposition rate of host was controlled at 0.2 nm s⁻¹, and the deposition rate of the dopant was adjusted according to the volume ratio doped in the host materials. The electroluminescence (EL) and current density-voltage(*J-V*) characteristics of the devices were measured by a constant current source (Keithley 2400 SourceMeter) combined with a photometer (Photo Research SpectraScan PR655).

Synthesis:

The compound **2** was synthesized according to our previous literature^[1].



Scheme S1 Synthetic route of 2P-BT-N-2TPA and 2TPA-BT-N-2P

Synthesis of compound 2P-NH2.

A mixture of **2** (2.0 g, 6.47 mmol), 4-Bromotriphenylamine (2.4 g, 7.26 mmol), aqueous K_2CO_3 (2.0 M, 13 mL) and $\text{Pd(PPh}_3)_4$ (0.4 g, 0.32 mmol) in 100 mL toluene was stirred for 24 h at $90\text{ }^\circ\text{C}$ under a nitrogen atmosphere. After cooled to RT, the mixture was extracted with dichloromethane (4×45 mL), and the combined organic layer was dried over anhydrous MgSO_4 . The solvent was removed off by rotary evaporation and the residue was passed through a flash silica gel column using petroleum ether/ dichloromethane (v/v, 3:2) as an eluent to obtain **2P-NH2** as light green solid (1.4 g, 71.4%). ^1H NMR (600 MHz, CD_2Cl_2) δ 7.93 (d, $J = 7.2\text{ Hz}$, 2H),

7.52 (ddt, $J = 16.7, 14.7, 7.1$ Hz, 7H), 7.33 (s, 1H), 4.30 (s, 2H). ^{13}C NMR (151 MHz, CD_2Cl_2) δ 156.59, 149.29, 144.14, 137.18, 135.07, 133.48, 130.25, 129.13, 128.95, 128.37, 127.93 – 127.85, 127.58, 122.95, 111.17.

Synthesis of compound **2P-BT-N-2TPA**.

A mixture of **2P-NH₂** (1.0 g, 3.30 mmol), phenylboronic acid (1.7 g, 14.24 mmol), aqueous Potassium tert-butoxide (2.0 g, 19.8 mmol), Palladium (II) Acetate (0.40 g, 0.17 mmol) and (*t*-Bu)₃ P. HBF₄ (0.50 g, 0.17 mmol) in 100 mL toluene was stirred for 24 h at 110 °C under a nitrogen atmosphere. After cooled to RT, the mixture was extracted with dichloromethane (4×45 mL), and the combined organic layer was dried over anhydrous MgSO₄. The solvent was removed off by rotary evaporation and the residue was passed through a flash silica gel column using petroleum ether/dichloromethane (v/v, 1:1) as an eluent to obtain **2P-BT-N-2TPA** as red solid (1.0 g, 38.4%). ^1H NMR (400 MHz, CDCl_3) δ 7.89 (d, $J = 7.8$ Hz, 2H), 7.72 (s, 1H), 7.58 – 7.51 (m, 2H), 7.47 (dd, $J = 8.3, 6.3$ Hz, 1H), 7.39 (d, $J = 7.6$ Hz, 2H), 7.37 – 7.26 (m, 4H), 7.22 (d, $J = 7.4$ Hz, 7H), 7.15 – 6.65 (m, 20H). ^{13}C NMR (101 MHz, CD_2Cl_2) δ 157.07, 151.94, 147.84, 142.39, 137.04, 135.77, 133.51, 130.19, 129.16, 128.48, 127.88, 127.36, 125.72, 123.92, 123.39, 122.23. MALDI-MS (m/z) of $\text{C}_{54}\text{H}_{39}\text{N}_5\text{S}$ for $[\text{M}^+]$: calcd. 790.00; found, 789.06.

Synthesis of compound **2TPA-NH₂**.

The synthesis method of **2TPA-NH₂** is consistent with **2P-NH₂** and get yellow solid as yields up to 83.5%. ^1H NMR (600 MHz, CD_2Cl_2) δ 7.85 (d, $J = 8.6$ Hz, 2H), 7.48 (d, $J = 8.5$ Hz, 2H), 7.36 – 7.26 (m, 9H), 7.19 (dd, $J = 17.6, 9.5$ Hz, 12H), 7.08 (dd, J

= 13.3, 7.1 Hz, 4H), 4.34 (s, 2H). ^{13}C NMR (151 MHz, CD_2Cl_2) δ 156.71, 149.41, 148.09, 147.52, 147.20, 144.32, 132.62, 130.97, 130.65, 129.85, 129.30, 128.57, 124.74, 123.54 – 122.96, 122.63, 122.03, 110.49.

Synthesis of compound 2TPA-BT-N-2P.

The synthesis method of **2TPA-BT-N-2P** is consistent with **2P-BT-N-2TPA** and get orange solid as yields up to 74.3%. ^1H NMR (600 MHz, CD_2Cl_2) δ 7.79 (d, J = 8.6 Hz, 2H), 7.61 (s, 1H), 7.52 – 6.71 (m, 36H). ^{13}C NMR (151 MHz, CD_2Cl_2) δ 156.94, 152.11, 148.17, 147.37, 146.90, 145.20, 132.84, 130.55, 129.78, 129.29, 129.07, 128.95, 127.69, 124.42, 123.33, 122.71, 122.54, 122.23. MALDI-MS (m/z) of $\text{C}_{54}\text{H}_{39}\text{N}_5\text{S}$ for $[\text{M}^+]$: calcd. 790.00; found, 789.06.

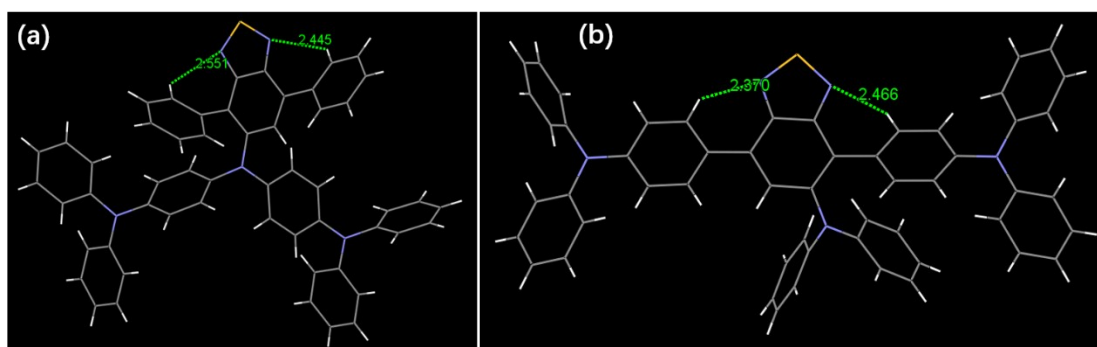


Fig. S1 distance of the nitrogen atoms in the benzothiadiazole group and hydrogen on the attached benzene ring for 2P-BT-N-2TPA and 2TPA-BT-N-2P

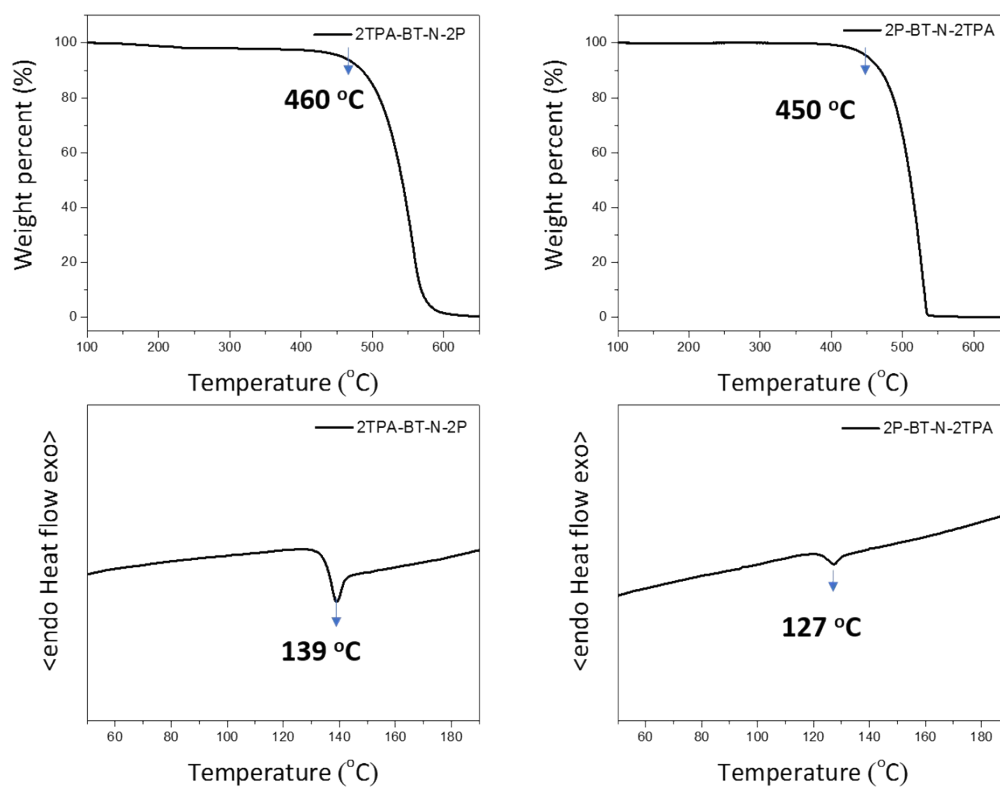


Fig. S2 TGA/DSC curves of 2P-BT-N-2TPA and 2TPA-BT-N-2P

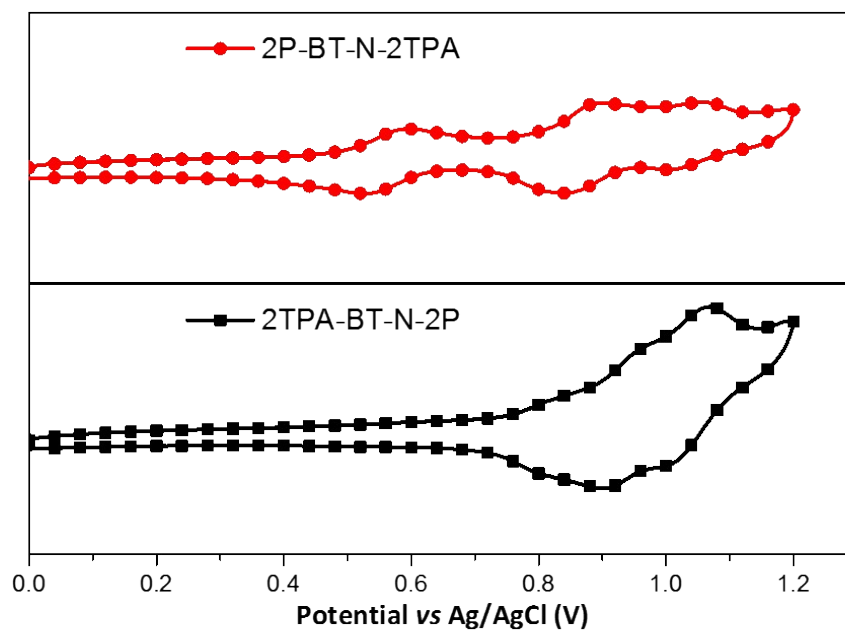


Fig. S3 CV curves of 2P-BT-N-2TPA and 2TPA-BT-N-2P

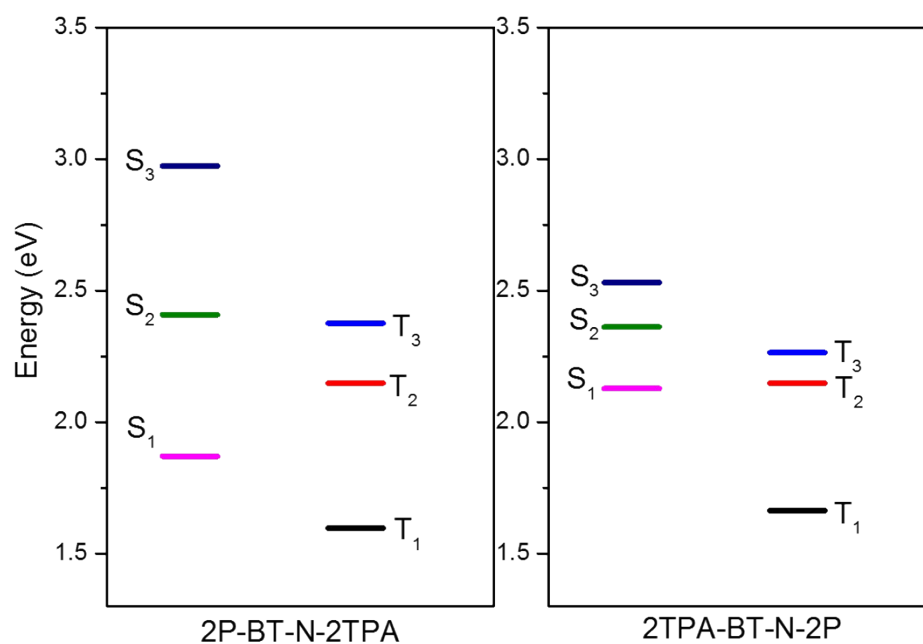


Fig. S4 Energy level of singlet (S) and triplet (T) states of 2P-BT-N-2TPA and 2TPA-BT-N-2P

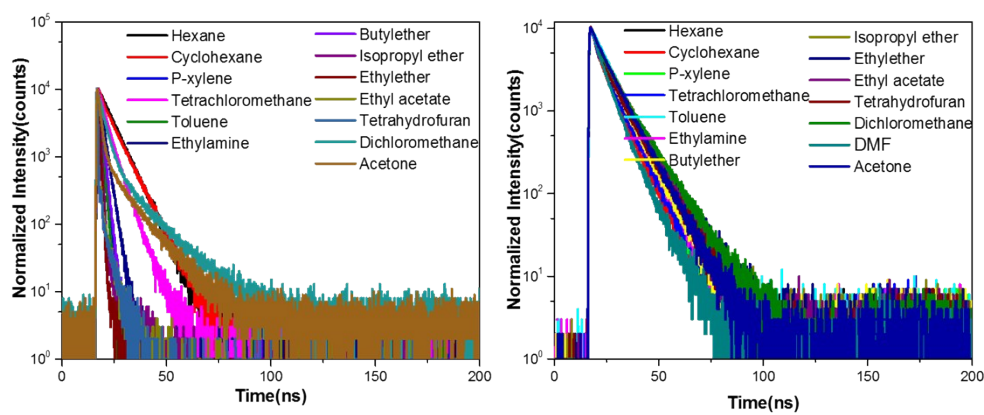


Fig. S5 Transient decay curves of 2P-BT-N-2TPA and 2TPA-BT-N-2P in different solvents

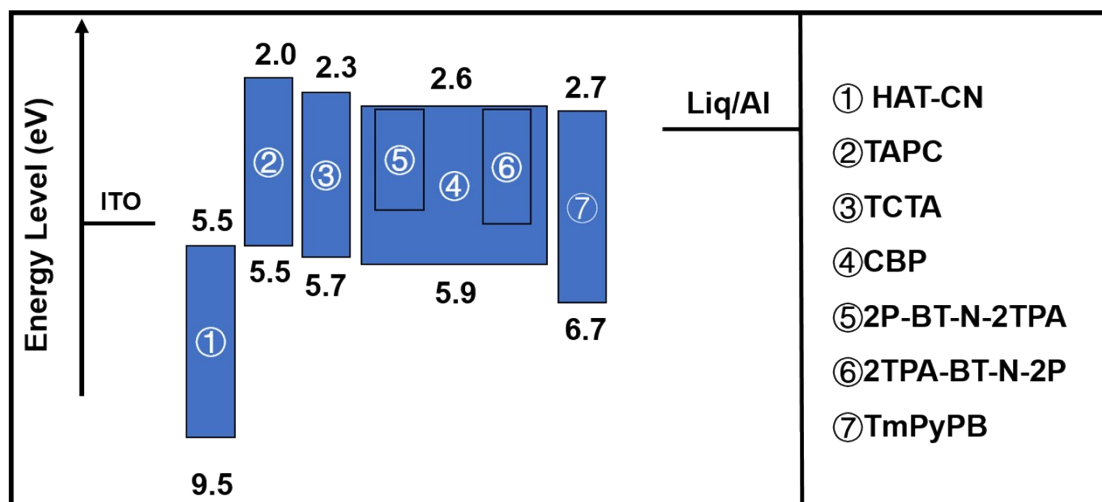


Fig. S6 Device structures of the 2P-BT-N-2TPA and 2TPA-BT-N-2P as well as the energy levels of used materials

Table S1 The values of intra/intermolecular interactions in crystalline for 2P-BT-N-2TPA and 2TPA-BT-N-2P

Compounds	2P-BT-N-2TPA	2TPA-BT-N-2P
Intramolecular interactions (Å)	C-H \cdots N-H: 2.445, 2.551, 2.684	C-H \cdots N-H: 2.370, 2.466, 2.654
	C-H $\cdots\pi$: 2.909~4.032	C-H $\cdots\pi$: 2.872~3.997
	C-H \cdots C-H: 2.823, 2.984, 3.086, 3.625, 3.268	C-H \cdots C-H: 2.137, 2.716, 2.777, 2.975, 3.113, 3.175, 3.393, 3.613
	$\pi\cdots\pi$: 3.037~3.939	$\pi\cdots\pi$: 3.087~3.907
Intermolecular interactions (Å)	C-H \cdots N-H: 2.821, 3.099, 3.947	C-H \cdots N-H: 3.156, 3.962
	C-H $\cdots\pi$: 3.137~4.125	C-H $\cdots\pi$: 2.740~4.161
	C-H \cdots C-H: 2.558, 2.675, 2.909, 3.180, 3.692, 3.856	C-H \cdots C-H: 2.764, 2.777, 2.797, 2.943, 3.050, 3.196, 3.212, 3.359, 3.457
	$\pi\cdots\pi$: 3.363	$\pi\cdots\pi$: 3.451

Table S2 Doping concentration dependent PLQY values for 2P-BT-N-2TPA and

2TPA-BT-N-2P		
Doping concentration (wt%)	PLQY of 2P-BT-N-2TPA (%)	PLQY of 2TPA-BT-N-2P (%)
2	0.14	0.84
5	0.20	0.90
10	0.17	0.93
15	0.15	0.95
20	0.13	0.95
100	0.11	0.91

References

1. H. Langhals, P. Knochel, A. Walter and Silvia Zimdars, *Synthesis*, 2012; **44**, 3465-3476.